Journal of Nuclear Medicine, published on December 22, 2022 as doi:10.2967/jnumed.122.264812

Distinguishing Progression from Pseudoprogression in Glioblastoma Using ^{18}F-Fluciclovine PET

Authors: Ali Nabavizadeh[1], Stephen J Bagley[2], Robert K Doot[1], Jeffrey B Ware[1], Anthony J Young[1], Satyam Ghodasara[1], Chao Zhao[3], Hannah Anderson[1], Erin Schubert[1], Erica L Carpenter[2], Jacob Till[2], Fraser Henderson Jr[4], Austin R Pantel[1], H Isaac Chen[5], John YK Lee[5], Nduka M. Amankulor[2,5], Donald M O'Rourke[2,5], Arati Desai[2], MacLean P Nasrallah[6], Steven Brem[2,5]

[1]Department of Radiology, Hospital of University of Pennsylvania, Perelman School of Medicine of the University of Pennsylvania, Philadelphia, Pennsylvania, 19104, USA
[2]Abramson Cancer Center, University of Pennsylvania, Philadelphia, PA, 19104, USA
[3] Department of Surgery, Children's Hospital of Philadelphia, Philadelphia, Pennsylvania, 19104, USA
[4]Department of Neurosurgery, Loma Linda University Medical Center, 11234 Anderson St, Loma Linda, CA 92354
[5]Department of Neurosurgery, Hospital of University of Pennsylvania, Perelman School of Medicine of the University of Pennsylvania, Philadelphia, Pennsylvania, USA
[6]Division of Neuropathology, Department of Pathology and Laboratory Medicine, Perelman School of Medicine, University of Pennsylvania, Philadelphia, PA, 19104, USA

Running title: ^{18}F-Fluciclovine PET in glioblastoma

Address correspondence:

Ali Nabavizadeh, M.D.
Assistant Professor of Radiology
Department of Radiology
1 Silverstein Building
Hospital of the University of Pennsylvania
3400 Spruce St.
Philadelphia, PA 19104
Email; Ali.Nabavizadeh@pennmedicine.Upenn.edu
Phone: 215-662-6865
Fax: 215-662-6865

Funding: Funding for this work was provided by Blue Earth Diagnostics to AN

Conflict of interest: AN received research funding (paid to the institution) from Blue Earth Diagnostics for this study. Other authors declare no potential conflicts of interest.

Word count: 3620

Abstract

Rationale:

Accurate differentiation between tumor progression (TP) and pseudoprogression remains a critical unmet need in neuro-oncology. ^{18}F-fluciclovine is a widely available synthetic amino acid PET radiotracer. In this study, we aimed to assess the value of ^{18}F-fluciclovine PET for differentiating pseudoprogression from TP in a prospective cohort of patients with suspected radiographic recurrence of glioblastoma

Methods: We enrolled 30 glioblastoma patients with radiographic progression after first-line chemoradiotherapy who were planned for surgical resection. Patients underwent pre-operative ^{18}F-fluciclovine PET and MRI. Relative percentages of viable tumor and therapy-related changes observed in histopathology were quantified and categorized as TP (≥50% viable tumor), mixed TP (<50% and >10% viable tumor), or pseudoprogression (≤10% viable tumor).

Results: Eighteen patients had TP, 4 mixed TP, and 8 pseudoprogression. Patients with TP/mixed TP had significantly higher 40-50 minutes SUVmax (6.64+ 1.88 vs 4.11± 1.52, p=0.009) compared to patients with pseudoprogression. A 40-50 minutes SUVmax cut-off of 4.66 provided 90% sensitivity and 83% specificity for differentiation of TP/mixed TP from pseudoprogression (Area under the curve (AUC)=0.86). Relative cerebral blood volume (rCBVmax) cut-off 3.672 provided 90% sensitivity and 71% specificity for differentiation of TP/mixed TP from Pseudoprogression (AUC=0.779). Combining a 40-50 minutes SUVmax cut-off of 4.66 and a rCBVmax cut-off of 3.67 on MRI provided 100% sensitivity and 80% specificity for differentiating TP/mixed TP from Pseudoprogression (AUC=0.95).

Conclusions: ^{18}F-fluciclovine PET uptake can accurately differentiate pseudoprogression from TP in glioblastoma, with even greater accuracy when combined with multi-parametric MRI. Given the wide availability of ^{18}F-fluciclovine, larger, multicenter studies are warranted to determine whether amino acid PET with ^{18}F-fluciclovine should be used in the routine assessment of post-treatment glioblastoma.

INTRODUCTION

Glioblastoma is the most common malignant primary brain tumor in adults and remains incurable following standard temozolomide-based chemoradiotherapy*(1).* Accurate assessment of tumor response and progression following treatment remains a significant clinical challenge in neuro-oncology, complicating both routine care and the conduct of clinical trials*(2).* Contrast-enhanced magnetic resonance imaging (MRI), the current standard for tumor monitoring, lacks specificity for detecting neoplastic progression in the brain. This is largely because contrast enhancement can increase due to any cause of blood-brain barrier breakdown and resultant contrast extravasation, including secondary to effective chemoradiotherapy*(3).* This phenomenon, referred to as pseudoprogression (pseudoprogression)*(4),* has been reported in up to 30% of patients after chemoradiotherapy as defined by the Response Assessment in Neuro-Oncology working group (i.e., within 12 weeks after completion of radiotherapy)*(5)*; however late pseudoprogression may also occur beyond 12 weeks*(6)*. Radiographic changes that occur 6 months to several years post-treatment, namely radiation necrosis*(7)*, also share common pathophysiological features with pseudoprogression*(7)*.

In post-treatment glioblastoma, accurate differentiation of pseudoprogression from true tumor progression (TP) represents a significant unmet clinical need, as erroneous interpretation can lead to premature discontinuation of an effective treatment and/or overestimation of the efficacy of subsequent salvage therapies*(8).* In addition, early recognition of tumor progression offers the possibility for earlier therapeutic interventions, such as re-resection or recruitment to experimental clinical trials, at a time in the disease course when patients are healthier overall and with relatively preserved performance status. While advanced MRI techniques such as dynamic susceptibility contrast (DSC), dynamic contrast-enhanced (DCE) and diffusion-weighted imaging (DWI) have improved the ability to differentiate pseudoprogression from TP, the application of these techniques in both routine practice and clinical trials has been hampered by considerable variability in acquisition and analysis approaches between institutions (9). In addition, these techniques have imperfect accuracy and are frequently affected by imaging artifacts, especially in post-treatment setting*(10).*

Metabolic imaging can provide additional valuable information about tumor status. In particular, positron emission tomography (PET) with amino acid tracers including ^{11}C-methionine (^{11}C-MET) (11), ^{18}F-fluorodopa (^{18}F-FDOPA)*(12)*, and 18F-fluoro-ethyltyrosine (^{18}F-FET)*(13,14)* have shown value in differentiating pseudoprogression from TP, as amino acid uptake is increased in tumor tissue but low in areas of treatment-related change. Recent expert reviews by the PET-Response Assessment in Neuro-Oncology group find amino acid tracers (^{11}C-MET, ^{18}F-FET, and ^{18}F-FDOPA) to have higher diagnostic accuracy than conventional and advanced MRI in the differentiation of glioma recurrence*(15, 16).*

^{18}F-Fluciclovine is a synthetic amino acid PET tracer approved by the US Food and Drug Administration (FDA) in the setting of biochemical recurrence of prostate cancer with an excellent safety profile*(17)*. ^{18}F-Fluciclovine is an isoleucine analogue that is transported into glial cells by both L-amino acid transporters (LATs; especially LAT1) and alanine–serine–cysteine transporters (ASCTs; especially ASCT2), which are up-regulated in glioma cells and demonstrate low expression in the normal brain parenchyma*(18)*. ^{18}F-Fluciclovine has also demonstrated utility for discrimination between low-grade and high-grade glioma*(19-22)*. In comparison with ^{11}C-MET in both treatment naïve and recurrent glioma, ^{18}F-fluciclovine demonstrated similar detection accuracy, but better contrast between tumor

and background uptake*(19)*. In contrast to ^{11}C-MET, which has a short half-life (20 min) and is limited to PET centers with a cyclotron*(19)*, ^{18}F-fluciclovine has the same longer half-life (109.8 min), as ^{18}F-FET and ^{18}F-FDOPA, which allows time for it to be shipped from the manufacturer to the imaging centers. In addition, unlike ^{18}F-FET and ^{18}F-FDOPA, ^{18}F-fluciclovine is widely available in the US given its usage in the setting of prostate cancer*(23)*. Our group previously demonstrated the feasibility of ^{18}F-fluciclovine PET-MRI guided biopsy in post-treatment glioblastoma to distinguish areas of highest tumor recurrence from areas of treatment-related changes in a small case series*(24)*. The aim of this study was to assess the independent and additive value of ^{18}F-fluciclovine PET and multi-parametric MRI for differentiating pseudoprogression from TP. Importantly, we utilized a study cohort in which all patients had available resected tumor tissue to serve as ground truth for TP vs. pseudoprogression.

MATERIALS AND METHODS

Study Design and Patient Population

We conducted a prospective cohort study (NCT03990285) of 30 adult patients with previously confirmed diagnosis of glioblastoma (defined according to the WHO 2021 Classification)*(25)* who were 1) previously treated with standard of care radiation and temozolomide and 2) scheduled to have surgery based on radiographic progression (i.e., new contrast-enhancing lesions or lesions showing ≥25% increase in the sum of the products of the perpendicular diameters on MRI) according to response assessment in Neuro-Oncology criteria*(26)*. Patients underwent pre-operative multi-parametric MRI and 60 minutes of dynamic brain PET-CT imaging after intravenous administration of ^{18}F-fluciclovine. Patients subsequently underwent maximal safe resection of the enhancing lesion. The percentages of viable tumor and therapy-related changes comprising the specimen were quantified on histopathology by a board-certified neuropathologist (M.P.N.) as detailed below. All patients provided written informed consent. This study was approved by the Institutional Review Board of the University of Pennsylvania.

Image Acquisition:

PET:

^{18}F-Fluciclovine (Axumin®; Blue Earth Diagnostics) was produced by PETNET Solutions facilities under U.S. Pharmacopeia–compliant procedures and was administered under an investigational new drug application exemption. All PET studies were performed on an Ingenuity TF PET/CT device (Philips Healthcare) using a previously described method of image reconstruction*(27)*. Patients underwent 60-minutes of dynamic PET imaging after injection of 191± 21 MBq of ^{18}F-fluciclovine. In 2 patients, PET acquisition was performed for 40 and 45 minutes instead of 60 minutes. Patients fasted for 4 hours before administration of ^{18}F-fluciclovine. Adverse events were recorded for the period up to 24 hours post each injection of the ^{18}F-fluciclovine radiotracer and no adverse events were observed.

MRI:

Brain MRI was performed using the brain tumor imaging protocol of the University of Pennsylvania on a 3 Tesla magnet (Trio, Siemens) which included axial T1-weighted 3D MPRAGE before and after contrast, post-contrast axial FLAIR, diffusion tensor imaging (DTI) (n=30), dynamic contrast-enhanced (DCE) perfusion (n=29), and dynamic susceptibility contrast (DSC) perfusion (n=27 after excluding 2 patients with degraded source data due to susceptibility effects). Representative imaging parameters are presented in supplementary table 1. Two contrast boluses (Gadoterate meglumine, Guerbet) with a

dose of 0.1 mmol/kg were sequentially administered for DCE followed by DSC imaging, with the dose administered for DCE serving as a preload dose for DSC to reduce the effect of contrast agent leakage on relative cerebral blood volume (rCBV) measurements.

Image Analysis:

PET:

PET measurements were performed in MIM (versions were updated throughout the study from 6.9 to 7.1). Volumes of interest (VOI) of resected tumor were defined using PET and co-registered to T1 postcontrast MRI and FLAIR sequences with placement confirmed by a board-certified neuroradiologist and nuclear radiologist (A.N.). Measurements were taken of tumor SUVmax, one cubic centimeter SUVpeak, and 50% threshold SUVmean defined on 20-30, 30-40, 40-50, 50-60, 40-60, and 30-60 minute post-injection summed images (g/mL units). Normal tissue VOIs and SUVmean measurements were made on contralateral normal brain, pituitary gland, and superior sagittal sinus (SSS). The contralateral normal brain VOIs were 20mm in diameter while the pituitary and SSS VOIs were 15mm in diameter. Tumor SUVs and SUVratios (SUVR) normalized to each normal tissue SUVmean were calculated.

Time-activity curves (TACs) of ^{18}F-fluciclovine SUVpeak uptake in the tumor were generated by application of a spherical volume-of-interest with a volume of 1 mL centered on maximal tumor uptake to the entire dynamic dataset. TACs of each lesion were visually assessed by an experienced board certified nuclear radiologist (A.N.) as previously described*(28)* and assigned to one of the following curve patterns: constantly increasing without identifiable peak uptake (pattern I); peaking at a mid-point followed by a plateau or a small descent (pattern II); and uptake peaking early followed by a constant descent (pattern III)*(28)*. In addition, Time-to-peak (TTP) with a lower threshold time ≥ 10-min was measured and compared between each group.

MRI:

Regions of abnormal contrast enhancement, necrosis, and non-enhancing FLAIR signal intensity were segmented using a semi-automated segmentation tool (ITKSNAP)*(29)* followed by manual editing by a board-certified neuroradiologists (A.N. and J.B.W.). DTI processing was performed with FSL*(30)* and included removal of non-brain tissue as well as correction for motion and eddy currents. Diffusion data were then fit to the tensor model, and whole-brain maps of apparent diffusion coefficient (ADC) maps were used in subsequent analysis.

DCE images were corrected for motion and non-brain tissue was removed using image processing tools available in FSL. DCE data were then analyzed using the extended Toft's model, as implemented by the ROCKETSHIP software package*(31)* in the MATLAB programming environment (2014a, MathWorks), to derive voxel-wise maps of the volume transfer constant Ktrans, plasma volume fraction Vp, extravascular extracellular volume fraction Ve, and washout rate constant of contrast agent from the EES to the intravascular space Kep defined as Kep = Ktrans/Ve. Due to the inconsistent availability of T1 mapping among subjects, a fixed pre-bolus T1 value (1000 ms) was used to transform signal intensity curves to contrast concentration curves in DCE analysis. DSC data were used to generate leakage-corrected CBV maps using the γ-variate function as implemented in NordicICE software (NordicNeuroLab). For each functional modality (DTI, DCE, DSC), a reference image derived from source data was used to compute a linear transformation from the functional space to the subject's T1

postcontrast MPRAGE using the Advanced Normalization Tools (ANTs) registration tool*(32)*. These transformations were then used to co-register all parameter maps to the anatomical space. DCE and DSC imaging metrics were normalized to the median value of an ROI placed in normal-appearing white matter by a board-certified neuroradiologist (J.B.W.) at the same slice levels as the abnormality. Subsequent statistical analysis was based on the mean and maximum rCBV and DCE metric values as well as the mean and minimum ADC values extracted from the intersection of the segmented contrast-enhancement and PET ROI.

Histopathologic Evaluation and Analysis of Molecular Markers

After resection, the surgically extracted tissue specimens were entirely fixed in 10% buffered formalin, routinely processed, and embedded in paraffin. Five-micrometer thick sections of each specimen were cut onto glass slides, stained with hematoxylin and eosin, and assessed by a board-certified neuropathologist (M.P.N., blinded to the pre-operative MRI and PET imaging data). The presence or absence of pseudo-palisading necrosis and microvascular proliferation (features of recurrent glioblastoma), the presence or absence of dystrophic calcification and vascular hyalinization, and the percentage of geographic necrosis (representative of treatment-related changes) were quantified. Proliferative activity was determined by quantification of the number of mitotic figures in 10 high-power fields and semi-quantitative assessment of Ki-67 proliferative index by immunostaining (mouse monoclonal, MIB-1, IR62661; Dako, Carpinteria, California). Based on the combined assessment of these features, the entire resected specimen was assigned a tumor percentage 0-100%. Patients were considered TP if viable tumor represented ≥ 50% of the resected specimen, mixed TP if < 50% and > 10%, and pseudoprogression if tumor represented ≤ 10%.

Statistical Methods

Given the number of PET (6 summed images and normalized to normal contralateral brain, pituitary, and SSS) and MRI variables were higher than the number of subjects, the least absolute shrinkage and selection operator (LASSO) was used to determine the variables most predictive of viable tumor percentage on histopathology. In addition to imaging variables, the clinical variables of age, sex, O-6-methylguanine methyltransferase (*MGMT*) promoter methylation status, and the duration from the end of first line radiotherapy to recurrent surgery were included in the LASSO analysis. The strengths of correlations between primary outcome and selected variables were assessed by Pearson's correlation or Point-biserial correlation (rpb). A receiver operating characteristic (ROC) curve was used to illustrate the diagnostic ability of a binary classifier system as its discrimination threshold was varied. The criteria for determination of the most appropriate cut-off value was based on the point on the curve with minimum distance from the left-upper corner of the unit square. Furthermore, the Leave-One-Out Cross-Validation (LOOCV) procedure was used to estimate the performance of LASSO regression model by making predictions on test data. The differences in PET uptake between different groups (TP/mixed TP vs pseudoprogression and TP vs pseudoprogression) were compared using Wilcoxon rank-sum exact test. Kruskal-Wallis test was used to compare time to peak (TTP) between different groups. Chi square test was performed to compare MGMT methylation status in patients with TP compared to pseudoprogression. An $\alpha = .05$ was used as the cutoff for significance. All the statistical analyses were computed using code written in R version 4.1.0 (R Foundation).

RESULTS:

Baseline characteristics of the study cohort are summarized in table 1. Histopathologic analysis revealed 18 patients with TP, 4 with mixed TP, and 8 with pseudoprogression. Tumor percentage ranged from 0-100% (median = 57.50%, SD=31.66) and Ki67 ranged from 1-70% (median = 10%, SD=13.38). In patients with TP, 8 of 18 patients (44%) had MGMT methylated tumors. In patients with pseudoprogression, 1 of 8 patients (13%) had MGMT methylated tumor. A chi square test revealed no statistically significant difference in the rate of MGMT methylation between patients with TP vs. those with pseudoprogression (p = 0.29). All patients in this study (100%) had IDH-wild type tumors. A detailed description of demographics, clinical symptoms at the time of radiographic progression, MGMT and IDH status and tumor percentage on histopathology was provided in supplementary table 2).

Correlation of ^{18}F-Fluciclovine PET and MRI Parameters with Histopathologic and Clinical Variables:

50-60 minutes 50% threshold SUV mean (r=0.54, p=0.004), 50-60 minutes 50% threshold SUV mean/SSS (r=0.55, p=0.003) and 40-50 minutes SUVmax/pituitary (r=0.51, p=0.008) had a positive correlation with viable tumor percentage on histopathology. Among the MRI parameters, only rCBVmax was selected by the LASSO analysis and had a positive correlation with tumor percentage (r= 0.49; p= 0.011). 40-50 minutes SUV peak had a positive correlation with Ki67 (r=0.38) and a trend towards significance (p=0.056). There was no correlation between tumor percentage and age, sex, *MGMT* promoter methylation status, time elapsed between end of radiation and the patient's reoperation, or prior radiotherapy dose.

Differentiation of TP/mixed TP from pseudoprogression

Analysis of 25 subjects who had all the PET and MRI parameters (Table 2) demonstrated that patients with histopathologically proven TP/mixed TP had higher 40-50 minutes SUVmax (Odds ratio (OR)=1.14, rpb=0.49, p=0.011), 40-50 minutes SUVmax/pituitary (OR=1.43, rpb=0.56, p=0.003). None of the PET variables normalized to normal brain were selected by the LASSO analysis. Among the MRI parameters, rCBVmax (OR=1.13, rpb=0.47, p=0.016) was higher in the TP/mixed TP groups compared to the pseudoprogression group. Other MRI parameters were not selected by the LASSO analysis.

Analysis of 28 subjects with available 0-60-minute dynamic acquisition demonstrated that 50-60 minutes 50% threshold SUV mean (OR=1.31, rpb=0.52, p=0.004), 40-50 minutes SUVmax (OR=1.20, rpb=0.50, p=0.005), 40-50 minutes SUVmax/pituitary (OR=1.01, rpb=0.47, p=0.010), and 20-30 minutes SUVmax (OR=1.12, rpb= 0.49, p=0.007) were all higher in the TP/mixed TP group compared to the Pseudoprogression group.

Patients who demonstrated TP/mixed TP had a significantly higher 40-50 minutes SUVmax (6.64± 1.88 vs 4.11± 1.52, p=0.009) and 20-30 minutes SUVmax (6.59±2.15 vs 3.89±1.30, p=0.002) compared to patients with histological pseudoprogression (Figure 1). An illustrative case in which ^{18}F-fluciclovine PET uptake correctly predicted TP, whereas rCBV on DSC perfusion MRI did not, is displayed in Figure 2.

Although the main purpose of this work was to differentiate patients with TP/mixed TP vs. pseudoprogression, an exploratory analysis was also performed to differentiate TP from pseudoprogression (Supplementary results, supplementary figure 1 and supplementary table 3).

ROC Analyses

20-30 minutes SUVmax cut-off of 4.457 provided 95% sensitivity and 83% specificity for differentiation of TP/mixed TP from pseudoprogression (AUC=0.902). 40-50 minutes SUVmax cut-off of 4.662 provided 90% sensitivity and 83% specificity for differentiation of TP/mixed TP from pseudoprogression (AUC=0.856). rCBVmax cut-off 3.672 provided 90% sensitivity and 71% specificity for differentiation of TP/mixed TP from pseudoprogression (AUC=0.779). Combining a 40-50 minutes SUVmax cut-off of 4.662 and an rCBVmax cut-off of 3.672 provided 100% sensitivity and 80% specificity for differentiating TP/mixed TP from pseudoprogression (AUC=0.95, figure 3). Similar AUC of 0.95 was obtained after combining 20-30 minutes SUVmax cut-off of 4.457 and rCBVmax cut-off of 3.672. Combining a 40-50 minutes SUVmax cut-off of 4.662 and rCBVmax cut-off of 3.672 applying leave one out cross-validation provided 100% sensitivity and 80% specificity for differentiation of TP/mixed TP from pseudoprogression. (AUC=0.800, supplementary figure 2).

PET Tracer Kinetics:

The TAC demonstrated accumulation at the tumor bed that reached a steady-state after 20 minutes (figure 4A). All patients except two demonstrated type II (plateau) pattern (figure 4B). One patient with TP and extra-cranial tumor extension to the overlying scalp demonstrated type III pattern. One patient with TP demonstrated type I pattern. The TTP was not different (p=0.830) between the groups (figure 4C). Representative patients from TP, TP/mixed TP and pseudoprogression are demonstrated in figure 5.

DISCUSSION:

In this study, we demonstrated that ^{18}F-fluciclovine PET can accurately differentiate pseudoprogression from TP/mixed TP in glioblastoma patients following chemoradiotherapy. The accuracy of ^{18}F-fluciclovine PET in our study is in the higher range of prior studies using ^{18}F-FET and ^{18}F-FDOPA and higher compared to ^{11}C-MET PET*(13, 14, 16, 28, 33-41)*. In addition, we demonstrated that ^{18}F-fluciclovine PET has higher accuracy compared to advanced MRI sequences and that combining ^{18}F-fluciclovine PET with DSC perfusion MRI resulted in even better performance for differentiation between TP/mixed TP and pseudoprogression. A recent study of 21 patients with suspected recurrent high-grade glioma who received ^{18}F-fluciclovine PET imaging*(42)* demonstrated high median lesion-to-background ratio (42); however, no patients with confirmed pseudoprogression were included. To the best of our knowledge, our study is the first report that demonstrates the ability of ^{18}F-fluciclovine PET to discriminate between TP and pseudoprogression. We also found a positive correlation between Ki67 and PET parameters, which is consistent with a previous ^{18}F-fluciclovine study in biopsy-proven low- and high-grade gliomas (20) and a report of ^{18}F-fluciclovine PET-MR guided biopsy in a patient with treatment-naive oligodendroglioma*(21)*.

Although multi-parametric MRI including post-contrast imaging is widely used for surveillance of post-treatment glioblastoma, differentiation of pseudoprogression from TP using MRI is challenging as both of these entities may disrupt the blood-brain barrier (BBB) and lead to contrast extravasation and enhancement*(43)*. Amino acid PET imaging enables analysis of the tumor environment beyond disruption of the BBB because it is based on upregulation of amino acid transporters in the tumor cells (independent of BBB disruption)*(44-46)*. In addition, chronic blood products in the surgical bed cause susceptibility artifact and interfere with advanced MRI techniques such as DSC perfusion imaging, frequently confounding studies in post-treatment glioblastoma patients. In our study, DSC perfusion images were non-diagnostic in 2 patients and had to be excluded. Multiple studies compared the diagnostic accuracy of ^{18}F-FET PET and DSC perfusion MRI, and the results ranged from superior performance of PET to equal performance of both modalities*(34,47-49)*. Added value of PET and DSC perfusion was observed in some studies*(34,48,49)*, but these consisted of heterogeneous cohorts of grade 2-4 gliomas, and the final diagnosis was based on histology only in a subset of patients. Our results showed an accuracy of DSC MR imaging comparable to that observed in prior studies, and multi-parametric analysis of PET and MRI provided improved accuracy in our study, consistent with prior ^{18}F-FET studies*(34, 47, 49)*.

Unlike other amino acid PET agents, we found that absolute SUV measurements are more accurate for differentiating pseudoprogression from TP compared to normalized tumor to brain ratios, which is secondary to very low normal brain uptake and variability of normal brain uptake between patients. Conversely, normalization of SUVmax to pituitary gland showed similar accuracy to SUV max in differentiation of TP-mixed TP from pseudoprogression. Previous studies with ^{18}F-FET demonstrated the usefulness of TAC with curve pattern II or III and TTP<45 min for differentiating patients with TP from treatment-related changes*(34,35,50)*. In our study, we did not find TTP and TAC curve patterns to be useful as almost all patients demonstrated type II (plateau) pattern, consistent with a prior study in pretreatment glioma*(17)*. One patient with extra-cranial tumor extension to the overlying scalp demonstrated a type III pattern (uptake peaking early followed by a constant descent), similar to the described literature in prostate cancer*(51)*.

Our study has limitations, including the single-institution nature of the study which warrant future multicenter prospective studies to validate the generalizability of our findings. However, the prospective design, availability of histopathological confirmation in all patients, and short time interval between ^{18}F-fluciclovine PET and surgery are unique strengths compared to the majority of prior studies of amino acid PET tracers, which have been largely retrospective and have relied on the clinical follow-up to diagnose TP vs. pseudoprogression in most patients. In this study, all patients underwent dynamic PET imaging over 60 minutes Given that the uptake plateaus after 20 minutes and the high accuracy of both 20-30 and 40-50 minutes SUVmax, static imaging with both of these imaging windows can be used in clinical practice depending on the preference of the center. Of note, given the significant uptake of the radiotracer when compared to normal brain parenchyma in all patients (figure 5), quantitative criteria and not visual analysis alone are needed to differentiate between TP and pseudoprogression. Overall, our results suggest that ^{18}F-fluciclovine PET imaging can accurately differentiate pseudoprogression from TP in glioblastoma patients. Given the wide availability of ^{18}F-fluciclovine, larger, multicenter studies are warranted to determine whether amino acid PET imaging with ^{18}F-fluciclovine should be used in the routine assessment of post-treatment glioblastoma.

DISCLOSURE

AN received research funding (paid to the institution) from Blue Earth Diagnostics for this study.

KEY POINTS

Can 18F-Fluciclovine PET distinguishing progression from pseudoprogression in glioblastoma?

Our prospective study demonstrated that 18F-Fluciclovine PET uptake correlated with tumor percentage on histology and can distinguish progression from pseudoprogression in glioblastoma.

Given the wide availability of 18F-fluciclovine in US as an FDA approved radiotracer, this study has immediate translational relevance.

REFERENCES:

1. Stupp R, Mason WP, van den Bent MJ, et al. Radiotherapy plus concomitant and adjuvant temozolomide for glioblastoma. *N Engl J Med*. 2005;352:987-996.

2. Ellingson BM, Wen PY, Cloughesy TF. Modified criteria for radiographic response assessment in glioblastoma clinical trials. *Neurotherapeutics*. 2017;14:307-320.

3. Hygino da Cruz LC, Jr., Rodriguez I, Domingues RC, Gasparetto EL, Sorensen AG. Pseudoprogression and pseudoresponse: Imaging challenges in the assessment of posttreatment glioma. *AJNR Am J Neuroradiol*. 2011;32:1978-1985.

4. Langen KJ, Galldiks N, Hattingen E, Shah NJ. Advances in neuro-oncology imaging. *Nat Rev Neurol*. 2017;13:279-289

5. Wen PY, Chang SM, Van den Bent MJ, Vogelbaum MA, Macdonald DR, Lee EQ. Response assessment in neuro-oncology clinical trials. *J Clin Oncol*. 2017;35:2439-2449.

6. Kebir S, Fimmers R, Galldiks N, , et al. Late pseudoprogression in glioblastoma: Diagnostic value of dynamic o-(2-[18f]fluoroethyl)-l-tyrosine PET. *Clin Cancer Res*. 2016;22:2190-2196

7. Ellingson BM, Chung C, Pope WB, Boxerman JL, Kaufmann TJ. Pseudoprogression, radionecrosis, inflammation or true tumor progression? Challenges associated with glioblastoma response assessment in an evolving therapeutic landscape. *J Neurooncol*. 2017;134:495-504.

8. Reardon DA, Weller M. Pseudoprogression: Fact or wishful thinking in neuro-oncology? *Lancet Oncol*. 2018;19:1561-1563.

9. Patel P, Baradaran H, Delgado D, et al. MR perfusion-weighted imaging in the evaluation of high-grade gliomas after treatment: A systematic review and meta-analysis. *Neuro Oncol*. 2017;19:118-127

10. van Dijken BRJ, van Laar PJ, Smits M, Dankbaar JW, Enting RH, van der Hoorn A. Perfusion MRI in treatment evaluation of glioblastomas: Clinical relevance of current and future techniques. *J Magn Reson Imaging*. 2019;49:11-22.

11. Terakawa Y, Tsuyuguchi N, Iwai Y, et al. Diagnostic accuracy of 11C-methionine pet for differentiation of recurrent brain tumors from radiation necrosis after radiotherapy. *J Nucl Med*. 2008;49:694-699.

12. Chen W, Silverman DH, Delaloye S, et al. 18f-FDOPA PET imaging of brain tumors: Comparison study with 18F-FDG PET and evaluation of diagnostic accuracy. *J Nucl Med*. 2006;47:904-911.

13. Pöpperl G, Götz C, Rachinger W, Gildehaus FJ, Tonn JC, Tatsch K. Value of o-(2-[18F]fluoroethyl)-l-tyrosine PET for the diagnosis of recurrent glioma. *Eur J Nucl Med Mol Imaging*. 2004;31:1464-1470.

14. Rachinger W, Goetz C, Pöpperl G, et al. Positron emission tomography with o-(2-[18F]fluoroethyl)-l-tyrosine versus magnetic resonance imaging in the diagnosis of recurrent gliomas. *Neurosurgery*. 2005;57:505-511; discussion 505-511.

15. Albert NL, Weller M, Suchorska B, et al. Response assessment in neuro-oncology working group and european association for neuro-oncology recommendations for the clinical use of pet imaging in gliomas. *Neuro Oncol*. 2016;18:1199-1208.

16. Galldiks N, Niyazi M, Grosu AL, et al. Contribution of PET imaging to radiotherapy planning and monitoring in glioma patients - a report of the pet/rano group. *Neuro Oncol*. 2021;23:881-893

17. Kondo A, Ishii H, Aoki S, et al. Phase iia clinical study of [(18)F]fluciclovine: Efficacy and safety of a new pet tracer for brain tumors. *Ann Nucl Med*. 2016;30:608-618.

18. Shoup TM, Olson J, Hoffman JM, et al. Synthesis and evaluation of [18F]1-amino-3-fluorocyclobutane-1-carboxylic acid to image brain tumors. *J Nucl Med*. 1999;40:331-338.

19. Michaud L, Beattie BJ, Akhurst T, et al. (18)f-fluciclovine ((18)F-FACBC) PET imaging of recurrent brain tumors. *Eur J Nucl Med Mol Imaging*. 2020;47:1353-1367.

20. Parent EE, Benayoun M, Ibeanu I, et al. [(18)f]fluciclovine pet discrimination between high- and low-grade gliomas. *EJNMMI Res*. 2018;8:67.

21. Karlberg A, Berntsen EM, Johansen H, et al. Multimodal (18)F-fluciclovine PET/MRI and ultrasound-guided neurosurgery of an anaplastic oligodendroglioma. *World Neurosurg*. 2017;108:989.e981-989.e988.

22. Wakabayashi T, Iuchi T, Tsuyuguchi N, et al. Diagnostic performance and safety of positron emission tomography using (18)F-fluciclovine in patients with clinically suspected high- or low-grade gliomas: A multicenter phase iib trial. *Asia Ocean J Nucl Med Biol*. 2017;5:10-21.

23. Songmen S, Nepal P, Olsavsky T, Sapire J. Axumin positron emission tomography: Novel agent for prostate cancer biochemical recurrence. *J Clin Imaging Sci*. 2019;9:49.

24. Henderson F, Jr., Brem S, O'Rourke DM, et al. (18)F-fluciclovine pet to distinguish treatment-related effects from disease progression in recurrent glioblastoma: Pet fusion with mri guides neurosurgical sampling. *Neurooncol Pract*. 2020;7:152-157.

25. Louis DN, Perry A, Wesseling P, et al. The 2021 who classification of tumors of the central nervous system: A summary. *Neuro Oncol*. 2021;23:1231-1251.

26. Wen PY, Macdonald DR, Reardon DA, et al. Updated response assessment criteria for high-grade gliomas: Response assessment in neuro-oncology working group. *J Clin Oncol*. 2010;28:1963-1972

27. Kolthammer JA, Su KH, Grover A, Narayanan M, Jordan DW, Muzic RF. Performance evaluation of the ingenuity TF PET/CT scanner with a focus on high count-rate conditions. *Phys Med Biol*. 2014;59:3843-3859.

28. Galldiks N, Dunkl V, Stoffels G, et al. Diagnosis of pseudoprogression in patients with glioblastoma using o-(2-[18F]fluoroethyl)-l-tyrosine PET. *Eur J Nucl Med Mol Imaging*. 2015;42:685-695.

29. Yushkevich PA, Piven J, Hazlett HC, et al. User-guided 3D active contour segmentation of anatomical structures: Significantly improved efficiency and reliability. *Neuroimage*. 2006;31:1116-1128.

30. Smith SM, Jenkinson M, Woolrich MW, et al. Advances in functional and structural MR image analysis and implementation as FSL. *Neuroimage*. 2004;23 Suppl 1:S208-219.

31. Barnes SR, Ng TS, Santa-Maria N, Montagne A, Zlokovic BV, Jacobs RE. Rocketship: A flexible and modular software tool for the planning, processing and analysis of dynamic mri studies. *BMC Med Imaging*. 2015;15:19.

32. Avants BB, Epstein CL, Grossman M, Gee JC. Symmetric diffeomorphic image registration with cross-correlation: Evaluating automated labeling of elderly and neurodegenerative brain. *Med Image Anal*. 2008;12:26-41.

33. Mihovilovic MI, Kertels O, Hänscheid H, et al. O-(2-((18)F)fluoroethyl)-l-tyrosine pet for the differentiation of tumour recurrence from late pseudoprogression in glioblastoma. *J Neurol Neurosurg Psychiatry*. 2019;90:238-239.

34. Pyka T, Hiob D, Preibisch C,= et al. Diagnosis of glioma recurrence using multiparametric dynamic 18f-fluoroethyl-tyrosine pet-mri. *Eur J Radiol*. 2018;103:32-37.

35. Galldiks N, Stoffels G, Filss C, et al. The use of dynamic o-(2-18F-fluoroethyl)-l-tyrosine PET in the diagnosis of patients with progressive and recurrent glioma. *Neuro Oncol*. 2015;17:1293-1300.

36. Karunanithi S, Sharma P, Kumar A, et al. 18F-FDOPA PET/CT for detection of recurrence in patients with glioma: Prospective comparison with 18f-fdg pet/ct. *Eur J Nucl Med Mol Imaging*. 2013;40:1025-1035.

37. Minamimoto R, Saginoya T, Kondo C, et al. Differentiation of brain tumor recurrence from post-radiotherapy necrosis with 11c-methionine pet: Visual assessment versus quantitative assessment. *PLoS One*. 2015;10:e0132515.

38. Nihashi T, Dahabreh IJ, Terasawa T. Diagnostic accuracy of PET for recurrent glioma diagnosis: A meta-analysis. *AJNR Am J Neuroradiol*. 2013;34:944-950, s941-911.

39. Karunanithi S, Sharma P, Kumar A, Khangembam BC, Bandopadhyaya GP, Kumar R, et al. Comparative diagnostic accuracy of contrast-enhanced mri and (18)F-FDOPA PET-CT in recurrent glioma. *Eur Radiol*. 2013;23:2628-2635.

40. Werner JM, Weller J, Ceccon G, et al. Diagnosis of pseudoprogression following lomustine-temozolomide chemoradiation in newly diagnosed glioblastoma patients using FET-PET. *Clin Cancer Res*. 2021;27:3704-3713.

41. Salber D, Stoffels G, Pauleit D, et al. Differential uptake of o-(2-18F-fluoroethyl)-l-tyrosine, l-3h-methionine, and 3h-deoxyglucose in brain abscesses. *J Nucl Med*. 2007;48:2056-2062.

42. Bogsrud TV, Londalen A, Brandal P, et al. 18f-fluciclovine PET/CT in suspected residual or recurrent high-grade glioma. *Clin Nucl Med*. 2019;44:605-611.

43. Bagley SJ, Schwab RD, Nelson E, et al. Histopathologic quantification of viable tumor versus treatment effect in surgically resected recurrent glioblastoma. *J Neurooncol*. 2019;141:421-429.

44. Ono M, Oka S, Okudaira H, et al. Comparative evaluation of transport mechanisms of trans-1-amino-3-[^{18}F]fluorocyclobutanecarboxylic acid and l-[methyl-^{11}c]methionine in human glioma cell lines. *Brain Res*. 2013;1535:24-37.

45. Oka S, Okudaira H, Ono M, et al. Differences in transport mechanisms of trans-1-amino-3-[18f]fluorocyclobutanecarboxylic acid in inflammation, prostate cancer, and glioma cells: Comparison with l-[methyl-11C]methionine and 2-deoxy-2-[18F]fluoro-d-glucose. *Mol Imaging Biol*. 2014;16:322-329.

46. Scarpelli ML, Healey DR, Mehta S, Quarles CC. Imaging glioblastoma with (18)F-fluciclovine amino acid positron emission tomography. *Frontiers in oncology*. 2022;12:829050.

47. Verger A, Filss CP, Lohmann P, et al. Comparison of o-(2-(18)F-fluoroethyl)-l-tyrosine positron emission tomography and perfusion-weighted magnetic resonance imaging in the diagnosis of patients with progressive and recurrent glioma: A hybrid positron emission tomography/magnetic resonance study. *World Neurosurg*. 2018;113:e727-e737.

48. Jena A, Taneja S, Gambhir A, et al. Glioma recurrence versus radiation necrosis: Single-session multiparametric approach using simultaneous o-(2-18F-fluoroethyl)-l-tyrosine PET/MRI. *Clin Nucl Med*. 2016;41:e228-236.

49. Steidl E, Langen KJ, Hmeidan SA, et al. Sequential implementation of DSC-MR perfusion and dynamic [(18)F]FET PET allows efficient differentiation of glioma progression from treatment-related changes. *Eur J Nucl Med Mol Imaging*. 2021;48:1956-1965.

50. Werner JM, Stoffels G, Lichtenstein T, et al. Differentiation of treatment-related changes from tumour progression: A direct comparison between dynamic fet pet and adc values obtained from dwi mri. *Eur J Nucl Med Mol Imaging*. 2019;46:1889-1901.

51. Turkbey B, Mena E, Shih J, et al. Localized prostate cancer detection with 18F FACBC PET/CT: Comparison with MR imaging and histopathologic analysis. *Radiology*. 2014;270:849-856.

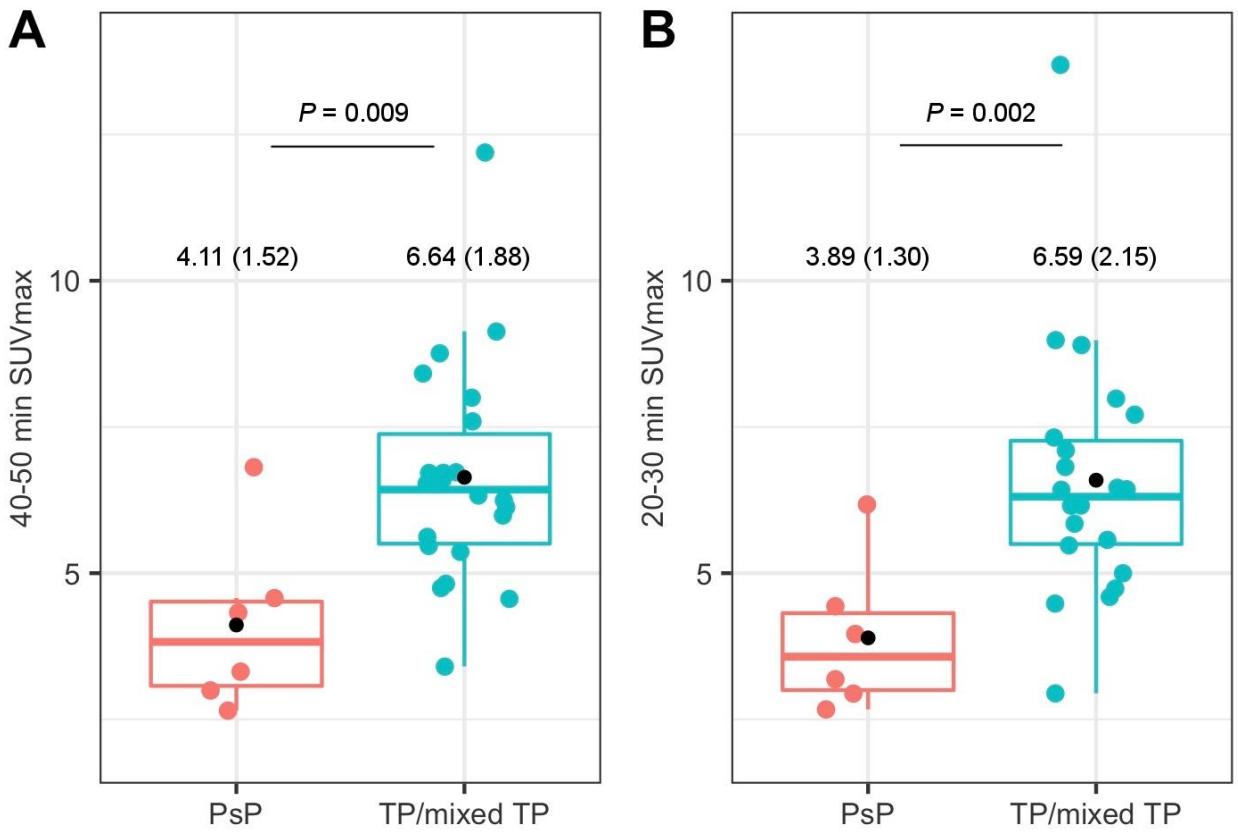

Figure 1. Comparison of PET parameters in patients with TP/mixed TP vs. pseudoprogression

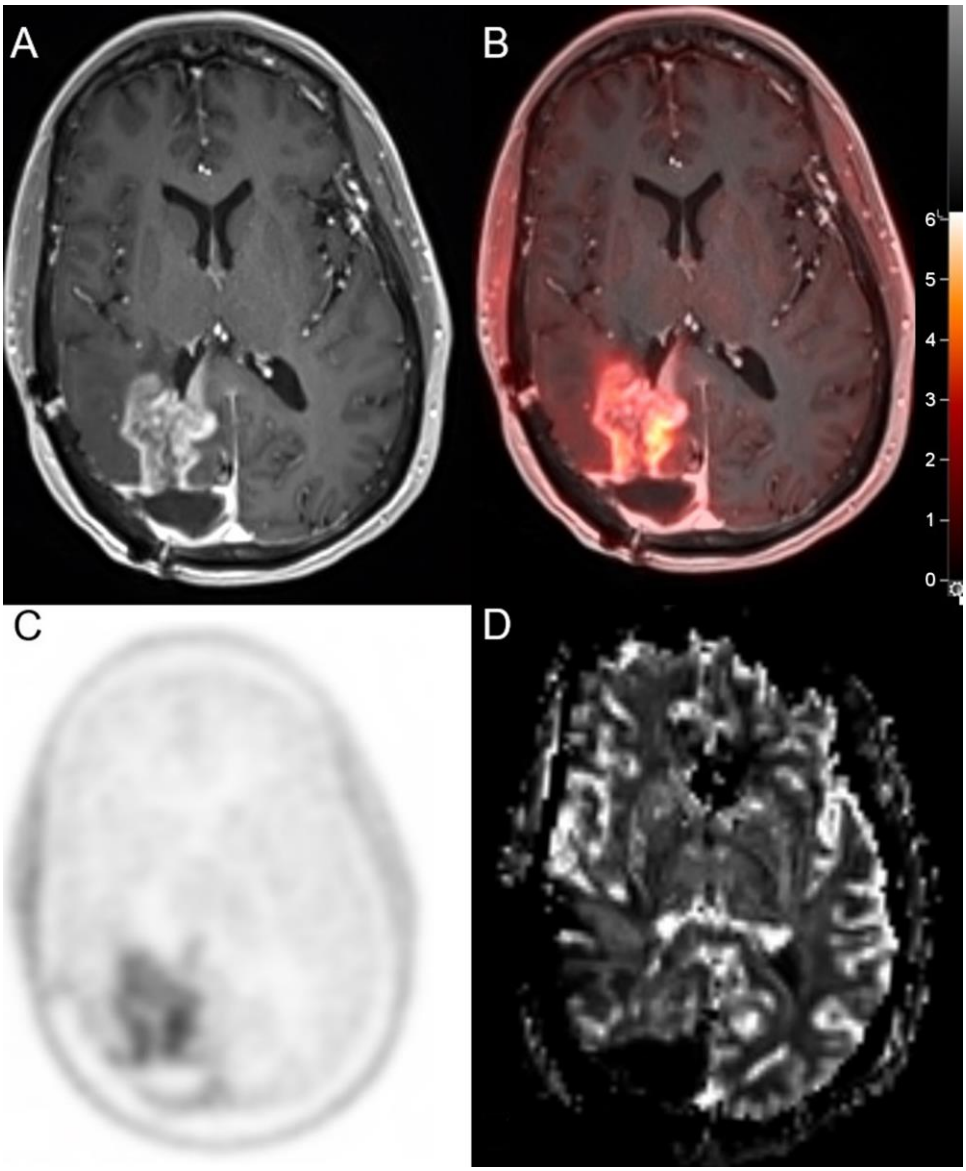

Figure 2. An example of false-negative MRI. A 65-year-old male with history of right occipital glioblastoma showed progressive enhancement adjacent to the resection cavity (A and B). ^{18}F-fluciclovine PET (C) imaging demonstrated marked increased radiotracer uptake (SUVmax=5.46) compared to only mild increase (rCBV=2.43) in rCBVmax on DSC perfusion MRI (D). Patient underwent resection and pathology showed that 60% of the specimen consisted of viable tumor and 40% consisted of therapy-related changes.

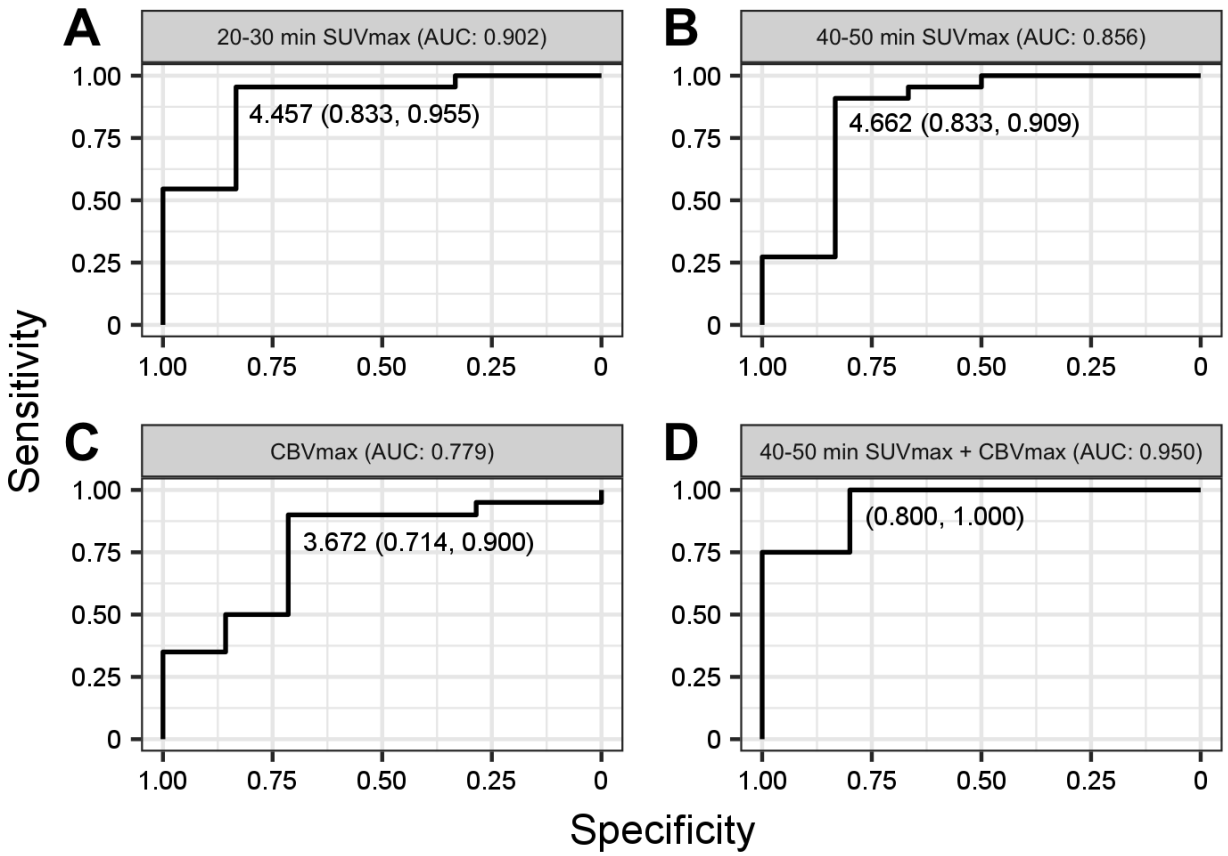

Figure 3. ROC analysis of 20-30 minutes SUVmax (A), 40-50 minutes SUVmax (B), CBVmax (C) and combined 40-50 minutes SUVmax-rCBVmax (D) to differentiate TP/mixed TP from pseudoprogression.

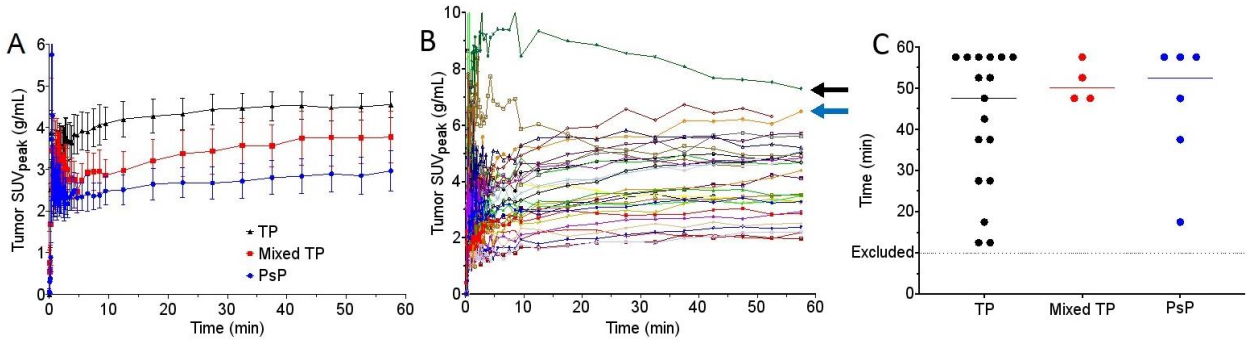

Figure 4. Comparison of mean time activity curves (TACs) (A) in patients with TP, mixed TP and pseudoprogression demonstrated accumulation at the tumor bed that reached a steady-state after 20 minutes. TACs in individual patients (B); all patients except two demonstrated type II (plateau) pattern. One patient with TP and extra-cranial tumor extension (black arrow) to the overlying scalp demonstrated type III pattern and one patient with TP demonstrated type I pattern (blue arrow). Comparison of mean time to peak (TTP) (C) in patients with TP, mixed TP and pseudoprogression.

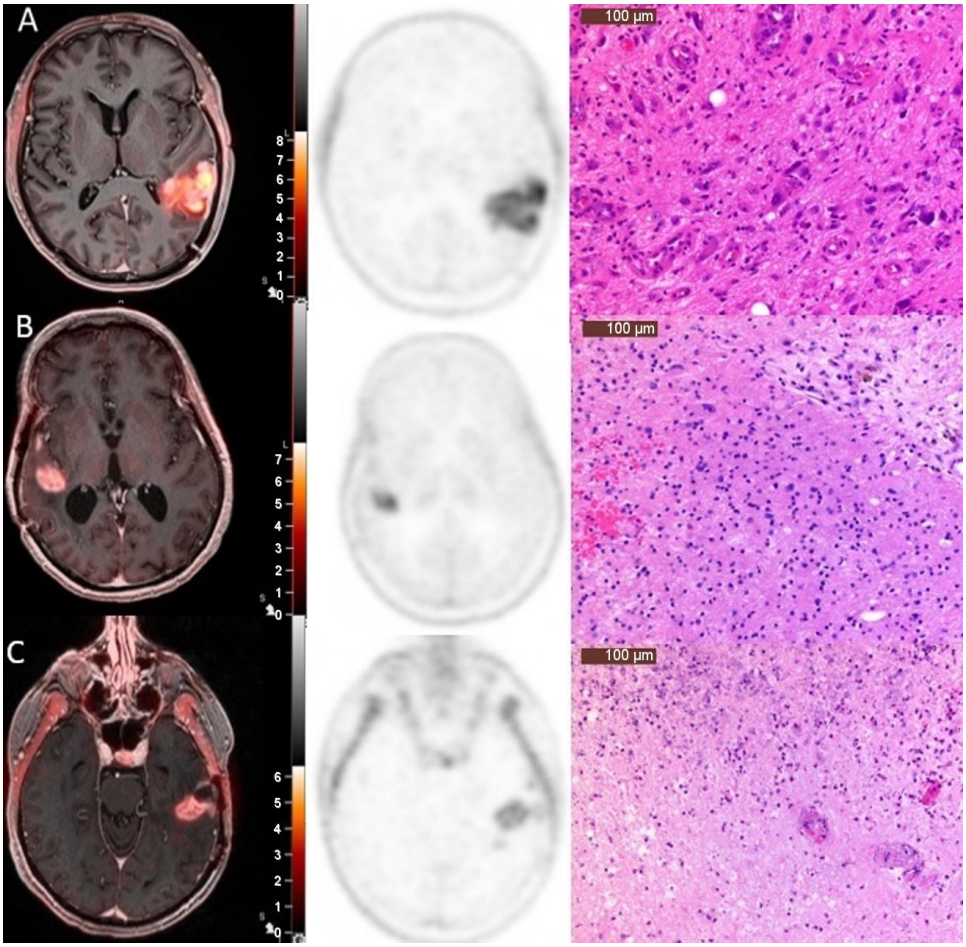

Figure 5. Imaging and histopathologic findings in 3 patients with true progression (A), mixed true progression-pseudoprogression (B) and pseudoprogression (C). A. 69-year-old female with history of left temporoparietal glioblastoma with progressive enhancement in the resection bed. 18F-fluciclovine PET imaging demonstrated marked increased radiotracer uptake (SUVmax=6.73). Patient underwent resection and pathology showed that histopathology demonstrates that most of the resected tissue is involved by atypical glial cells, consisting of both glial cells with enlarged, irregular, hyperchromatic nuclei consistent with recurrent glioma (Overall 80% tumor). B. A 64-year-old female with history of right temporal glioblastoma with progressive enhancement in the resection bed. 18F-fluciclovine PET imaging demonstrated moderate increased radiotracer uptake (SUVmax=4.75). Histopathology demonstrates treatment-related changes and 40% infiltrating glioma throughout the specimen. C. A 65-year-old male with history of left temporal glioblastoma with progressive enhancement in the resection bed. 18F-fluciclovine PET imaging demonstrated only mild radiotracer uptake (SUVmax=2.65). Histopathology demonstrates abundant treatment-related changes with no tumor throughout the specimen.

Baseline Characteristics	**Full Study Population N=30**
Sex, n (%)	
Male	10 (33.3)
Female	20 (66.7)
Age	
Median (Range)	62 (31 – 81)
MGMT Status, n (%)	
Pos (methylated)	10 (33.3)
Neg (unmethylated)	19 (63.3)
Unknown	1 (3.3)
Dose of first-line RT received, n (%)	
40 Gy	6 (20)
60 Gy	22 (73.3)
75 Gy	2 (6.7)
Weeks between completion of RT and surgery for recurrent glioblastoma Median (Range)	31.7 (5 – 283)
Days between PET scan and surgery for recurrent glioblastoma Median (Range)	4 (1 – 13)

Table 1. Demographics and clinical characteristics of patients

Variable selected for differentiation of TP/mixed TP from pseudoprogression	Odds ratio	Point-biserial correlation	p-value
40-50min SUVmax	1.14	0.49	0.011
40-50 minutes SUVmax/pituitary	1.43	0.56	0.003
rCBVmax	1.13	0.47	0.016

Table 2. Analysis of PET and MRI parameters for differentiation of TP/mixed TP from pseudoprogression

Graphical abstract

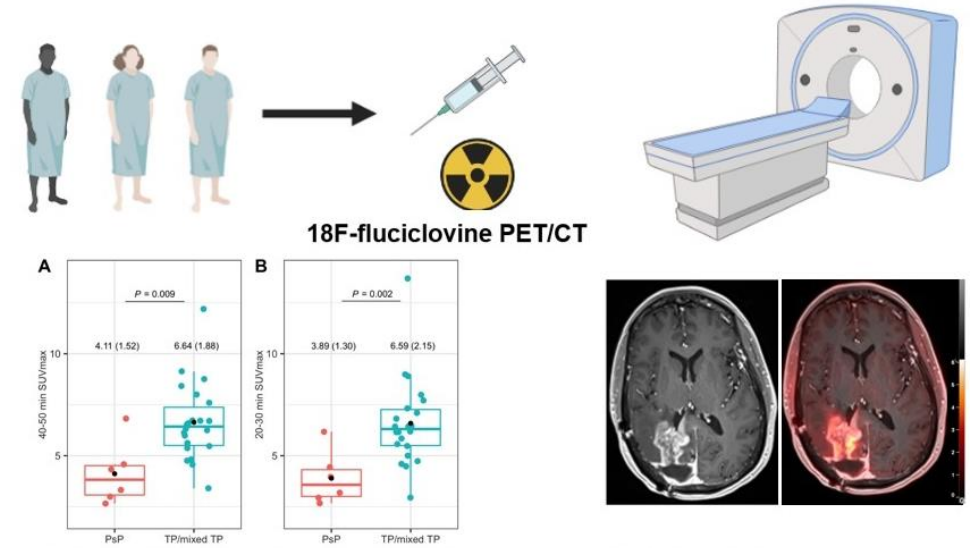

Implication: 18F-fluciclovine PET/CT uptake can accurately differentiate pseudoprogression from true progression in glioblastoma

Supplementary results:

Differentiation of TP from PsP

Analysis of 21 subjects with TP or PsP who had all the PET and MRI parameters (supplementary table 2) demonstrated that 40-60 minutes 50% threshold SUV mean (OR= 1.37, rpb=0.56, p=0.007) and 40-50 minutes SUVmax/pituitary (OR=1.37, rpb=0.61, p=0.002) were higher in the TP compared to PsP group. None of the PET variables normalized to normal brain were selected by the LASSO analysis. Among MRI parameters, rCBVmax (OR=1.08, rpb=0.50 p=0.018) and Vp mean (OR=1.49, rpb=0.55, p=0.009) were also higher in the TP compared to PsP group.

LASSO analysis of PET parameters demonstrated that 40-50 minutes SUVmax/pituitary (OR=1.12, rpb=0.52, p=0.008), 30-40 minutes SUVmax/pituitary (OR=1.05, rpb=0.51, p=0.009), 20-30 minutes SUVmax (OR=2.50, rpb=0.54, p=0.005), were higher in the TP compared to PsP group.

Patients who demonstrated TP had a significantly higher 40-50 minutes SUV max/pituitary (4.44±1.27 vs 2.79±1.03; p=0.009) and 20-30 minutes SUVmax (6.84 ± 2.21 vs 3.89+1.30, p=0.002) compared to patients with PsP (supplementary figure 1).

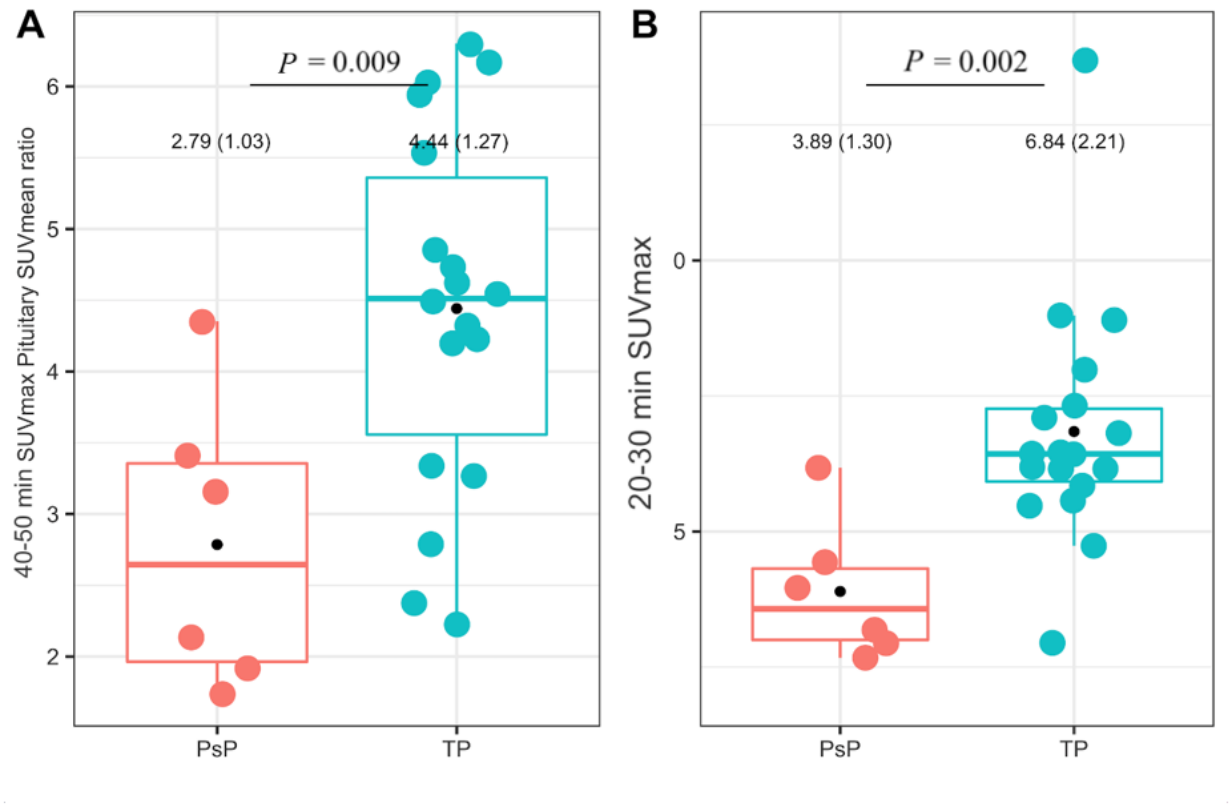

Supplementary figure 1. Comparison of PET parameters in patients with TP vs. PsP

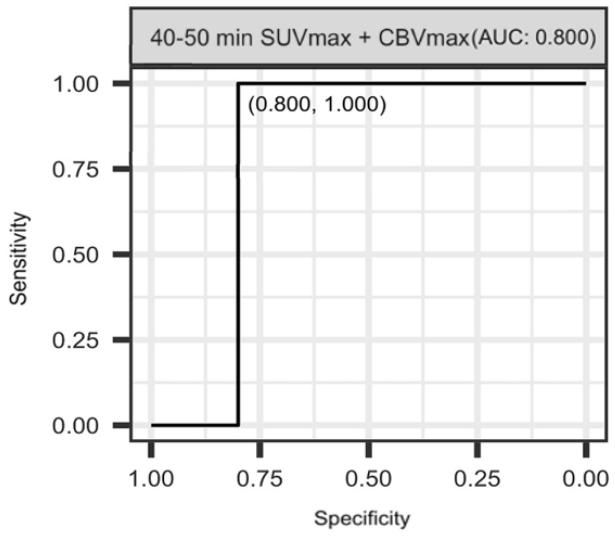

Supplementary figure 2. ROC analysis combining 40-50 minutes SUVmax cut-off of 4.662 and rCBVmax cut-off of 3.672 applying leave one out cross-validation to differentiate TP/mixed TP from PsP.

	TR (ms)	TE (ms)	TI (ms)	FA (^{0})	Spatial Resolution (mm)	Temporal Resolution (s)	B values (s/mm^2)	Gradient Directions
T1 MPRAGE	1730	2.75	900	9	0.5 x 0.5 x 1	-	-	-
FLAIR	10003	137	2550	150	0.94 x 0.94 x 3	-	-	-
DTI	6.7	95	-	90	1.88 x 1.88 x 3	-	0, 1000	30
DCE	7.06	1.57	-	23	0.86 x 0.86 x 3.5	7 (total 3.5 min)	-	-
DSC	1.5	35	-	60	1.8 x 1.8 x 4	1.5 (total 3 min)	-	-

Supplementary table 1. MRI imaging parameters

Subject	Age	Sex	Number of adjuvant Temozolomide cycles	Clinical symptoms at time of radiographic progression	MGMT status	IDH status	Tumor percentage on histology
1	62	F	6	Seizures	Unmethylated	Wild	30
2	64	F	5	Headache	Unmethylated	Wild	10
3	60	F	12	Transient episodes of RLE numbness	Unmethylated	Wild	75
4	67	F	6	Increasing headaches.	Unmethylated	Wild	50
5	**81**	**F**	12	Nausea	Methylated	Wild	80
6	64	M	1	Headache	Unmethylated	Wild	70
7	54	F	5	Difficulty with balance and increasing fatigue	Unmethylated	Wild	90
8	53	M	6	Cognitive problems	Methylated	Wild	70
9	69	F	2	Word-finding and comprehension difficulty	Unmethylated	Wild	80
10	55	F	2	Seizures	Unmethylated	Wild	90
11	31	F	6	Headache	Unmethylated	Wild	75
12	65	M	6	Seizures	Unmethylated	Wild	70
13	57	F	6	Headaches, visual changes and gait instability	Unmethylate	Wild	1
14	59	F	2	Gait instability, and left-sided weakness	Methylated	Wild	10
15	58	F	6	Headache, subtle language difficulties and fine motor skill reduction	Unmethylated	Wild	10
16	52	M	2	Increasing headaches with poor memory	Methylated	Wild	20
17	78	M	2	Increasing confusion and gait instability.	Unmethylated	Wild	60
118	65	F	6	Headache	Methylated	Wild	100
19	64	F	12	Increasing fatigue	Methylated	Wild	55

20	46	M	4	Blurry vision	Unmethylated	Wild	15
21	68	F	2	Seizures. Intermittent word finding and fatigue	Unmethylated	Wild	70
22	65	M	7	Increasing memory issues	Indeterminate	Wild	0
23	74	M	2	Word-finding difficulties, increased anxiety, dizziness	Methylated	Wild	70
24	64	F	5	Increasing fatigue	Unmethylated	Wild	40
25	58	F	6	Increasing headaches and fatigue	Methylated	Wild	75
26	55	F	5	Headache	Methylated	Wild	50
27	65	M	7	Headache and forgetfulness	Unmethylated	Wild	10
28	49	F	5	Headache	Unmethylated	Wild	5
29	60	F	1	Headache	Methylated	Wild	60
30	70	F	4	Increasing fatigue and cognitive deficits	Unmethylated	Wild	10

Supplementary table 2. Demographics, clinical symptoms at the time of radiographic progression, MGMT and IDH status and tumor percentage on histopathology

Variable selected for differentiation of TP from PsP			
40-50 minutes SUVmax/pituitary	1.37	0.61	0.002
40-60 minutes 50% threshold SUV mean	1.37	0.56	0.007
rCBVmax	1.08	0.50	0.018
Vp mean	1.49	0.55	0.009

Supplementary table 3. Analysis of PET and MRI parameters for differentiation of TP from PsP